ChemComm

RSC Publishing

COMMUNICATION

View Article Online
View Journal | View Issue

Cite this: *Chem. Commun.*, 2013, **49**, 8486

Received 3rd May 2013,
Accepted 24th July 2013

DOI: 10.1039/c3cc43298j

www.rsc.org/chemcomm

Au/ZnS core/shell nanocrystals as an efficient anode photocatalyst in direct methanol fuel cells†

Wei-Ta Chen,‡ Yin-Kai Lin,‡ Ting-Ting Yang, Ying-Chih Pu and Yung-Jung Hsu*

Au/ZnS core/shell nanocrystals with controllable shell thicknesses were synthesized using a cysteine-assisted hydrothermal method. Incorporating Au/ZnS nanocrystals into the traditional Pt-catalyzed half-cell reaction led to a 43.3% increase in methanol oxidation current under light illumination, demonstrating their promising potential for metal/semiconductor hybrid nanocrystals as the anode photocatalyst in direct methanol fuel cells.

Hybrid nanocrystals composed of a metal and a semiconductor have received considerable attention in recent years because their unique physical and chemical properties may give rise to superior performance in catalytic, magnetic, electronic, and optoelectronic applications.[1–4] For photocatalysis application, the metal is usually immobilized on the surface of the semiconductor in order to suppress the metal aggregation and thus keep the catalytic activity.[5] Besides, metal introduction to the semiconductor can induce effective charge separation as well as lower the activation energy to favour the resultant photocatalysis.[6] Such a design is however prone to metal poisoning due to the accumulation of reaction species on the metal surface.[7] To settle the poisoning issue, a metal/semiconductor core/shell architecture in which the metal is encapsulated within the semiconductor is proposed and developed.

For metal/semiconductor core/shell nanocrystals, the photo-excited electrons of the semiconductor would preferentially transfer to the metal, simultaneously leaving photogenerated holes in the semiconductor domain to achieve charge separation.[8] The positively charged holes are highly oxidative and may further participate in redox reactions like dye degradation and methanol oxidation. Recent developments have enabled the use of illuminated semiconductor nanocrystals in direct methanol fuel cells (DMFCs) to boost the cell performance.[9] In such a photo-assisted fuel cell system, methanol oxidation at the anode is carried out electrocatalytically on a precious metal and photocatalytically on a semiconductor under light illumination, which effectively cuts down the precious metal loading yet still enhances the cell power output. As a result of the inherently high electron–hole recombination rate, the semiconductor alone usually exhibits low carrier utilization efficiency and therefore limited cell performance enhancement when incorporated in DMFCs. By introducing metal/semiconductor core/shell nanocrystals which show pronounced charge separation at the anode, the performance of DMFCs may be further boosted under light illumination.

As the typical wide-bandgap semiconductor, ZnS possesses a considerably high conduction band potential,[10] which ensures the fast electron transfer when put in contact with the metal and thus the pronounced charge separation. On the other hand, when Au comes in contact with the semiconductor, the hybrid composites may undergo charge equilibration resulting in a negative shift of the apparent Fermi level and the enhanced catalytic activity.[11] The combination of Au and ZnS is therefore expected to achieve remarkable performance in photocatalysis. In this work, we investigated the photocatalytic properties of Au/ZnS core/shell nanocrystals toward methanol oxidation and demonstrated their use as the anode photocatalyst in the half-cell reaction of DMFCs under light illumination. The samples were prepared using a L-cysteine-assisted hydrothermal approach described in our previous work with slight modifications.[12] Because of the pronounced charge separation that occurred at the interface of Au and ZnS, the as-prepared Au/ZnS nanocrystals surpassed pure ZnS nanocrystals and commercial ZnS powders in photooxidation of methanol into formaldehyde. When incorporating Au/ZnS nanocrystals in the traditional Pt-catalyzed half-cell reaction, a 43.4% increase in methanol oxidation current was attained under light illumination, revealing their promising potential as the anode photocatalyst in DMFCs.

Au nanoparticles with an average diameter of 18 nm were first prepared using the citrate reduction method.[13] By reacting the pre-synthesized Au nanoparticles with L-cysteine–Zn^{2+} complexes in the hydrothermal reaction, Au/ZnS nanocrystals with well-defined core/shell architecture were obtained. Fig. S1A† shows the typical transmission electron microscopy (TEM) images of the as-obtained products. The obvious contrast between the inner core and outer

Department of Materials Science and Engineering, National Chiao Tung University, Hsinchu, Taiwan 30010, Republic of China. E-mail: yhsu@cc.nctu.edu.tw; Tel: +886 3 5712121 ext. 55317

† Electronic supplementary information (ESI) available: Experimental details, TEM images, TEM-EDS analysis, XRD patterns, steady-state PL spectra, recycling results, XPS spectra, and CV data of the samples. See DOI: 10.1039/c3cc43298j

‡ These authors contributed equally to this work.

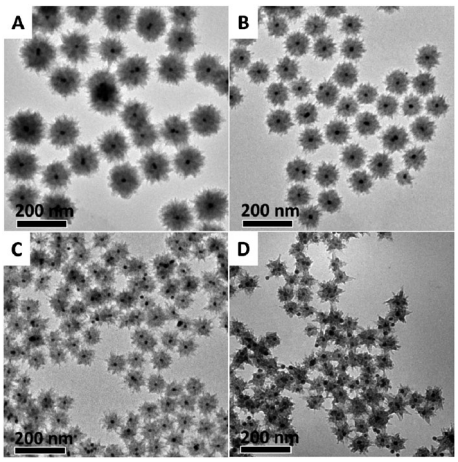

Fig. 1 TEM images of Au/ZnS nanocrystals prepared with Au of (A) 22.5, (B) 45, (C) 90, and (D) 180 μM. The samples are respectively denoted as Au/ZnS-1, Au/ZnS-2, Au/ZnS-3 and Au/ZnS-4.

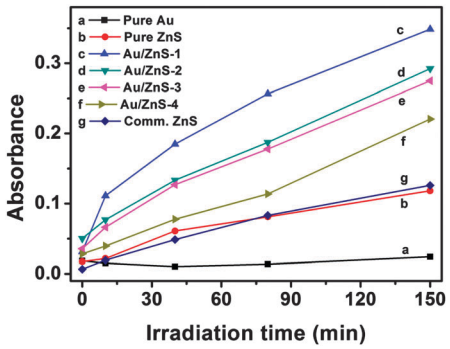

Fig. 2 Variation of DDL absorbance with irradiation time for different samples.

shell manifests the core/shell architecture of Au/ZnS. The high-resolution TEM image (Fig. S1B†), selected-area electron diffraction (SAED) (Fig. S1C†), energy dispersive spectrometer (EDS) analysis (Fig. S2†), and X-ray diffraction (XRD) (Fig. S3†) confirm the composition of Au and ZnS, and their crystallographic structures respectively as *fcc* and *wurtzite*.

Similar to the results obtained for Au/CdS core/shell nanocrystals,[12] the shell thickness of the present Au/ZnS nanocrystals can be readily controlled by modulating the relevant experimental parameters. Fig. 1 reveals the gradual decrease in shell thickness for Au/ZnS, which was achieved by adding Au nanoparticles of increasing concentrations. With increasing Au concentration, there are decreasing amounts of ZnS that can be formed on each of the Au nanoparticles, leading to the shrinking growth of the ZnS shell in the resulting Au/ZnS nanocrystals. From TEM observation, the shell thickness of Au/ZnS nanocrystals prepared with Au nanoparticles of 22.5, 45, 90, and 180 μM was estimated to be 53, 37, 29, and 22 nm, respectively.

Owing to the difference in band structure between Au and ZnS, the present Au/ZnS nanocrystals exhibited pronounced charge separation upon light irradiation, which was characterized by the depressed excitonic emission of ZnS (Fig. S4†). With the prevalence of charge carrier separation, abundant photogenerated holes were believed to exist and transfer to the shell surface of Au/ZnS nanocrystals, which may further react with water to produce $^{\bullet}OH$ radicals for photocatalysis application. In this work, the photooxidative conversion of methanol into formaldehyde was chosen as the test reaction to monitor the progress of photocatalysis for the samples.[14] When reacted with photogenerated holes and/or $^{\bullet}OH$ radicals, methanol undergoes oxidation to form formaldehyde.[15] The thus-formed formaldehyde can then react with acetylacetone and excess ammonium acetate to generate a yellow coloured product (diacetyldihydrolutidine, DDL) that can be quantitatively characterized by measuring its absorbance at 404 nm.[16] Fig. 2 represents the formation of DDL as a function of irradiation time over different samples. Note that experiments in the absence of the photocatalyst showed almost no DDL absorbance, suggesting that self-oxidation of methanol is negligible under light illumination. Since methanol itself was not oxidized in light, the vital DDL formation of the samples observed here was totally attributed to the outcome of methanol photooxidation. On the other hand, experiments in the presence of pure Au nanoparticles also showed negligible DDL absorbance, which excludes the concern about the possible contribution of pure Au toward methanol photooxidation. As evident from Fig. 2, all the four Au/ZnS samples performed better toward methanol photooxidation than pure ZnS nanocrystals and commercial ZnS powders, which was ascribed to the pronounced charge separation of Au/ZnS that caused the generation of abundant holes for methanol oxidation. Besides, Au/ZnS nanocrystals showed depressed photocatalytic efficiency as the ZnS shell thickness decreased. This phenomenon was attributed to the reduced amount of ZnS in the samples, with which less charge carriers were generated and thereby suppressed photocatalytic performance was attained. It should be mentioned that Au/ZnS with shell thickness larger than Au/ZnS-1 did not show accordingly higher photocatalytic efficiency. This could be ascribed to the relatively low ratio of Au loading that mitigated the overall charge separation as well as the essentially thick shell of ZnS that hindered the interfacial charge transfer. Furthermore, the results of the recycling test and X-ray photoelectron spectroscopy (XPS) analysis (Fig. S5 and S6†) reveal that the present Au/ZnS nanocrystals did not suffer from significant photocorrosion and exhibited considerably high stability during their use as a photocatalyst. The high stability of Au/ZnS possibly derived from the remaining carboxyl groups of L-cysteine at the nanocrystal surfaces, which may act as hole-transfer mediators to ease the hole accumulation on ZnS and thus moderate the photocorrosion.[17] A similar phenomenon has been observed in Au/CdS nanocrystals in which considerably high stability was also noticed.[12]

To explore the applicability of the present Au/ZnS nanocrystals in a more practical situation, their participation together with precious metal catalysts in the anodic half-cell reaction of DMFCs was demonstrated. Fig. 3 displays the cyclic voltammograms (CVs) of methanol oxidation recorded in alkaline media on commercial carbon-supported Pt (Pt/C) catalyst without and with the introduction of Au/ZnS nanocrystals. For the pristine Pt/C catalyst, two anodic peaks associated with methanol electrocatalysis were noticed. The peak at −0.15 V (*vs.* Ag/AgCl) in the forward scan corresponds to the methanol oxidation, while the peak appearing in the backward scan at −0.28 V arises from the removal of the CO species adsorbed on the catalyst surface. The value of the current of the forward peak can thus be regarded as a quantitative index for evaluating the efficiency of methanol electrocatalysis, which was estimated to be 287.7 mA mg^{-1} for pristine Pt/C. When employing Au/ZnS nanocrystals together with

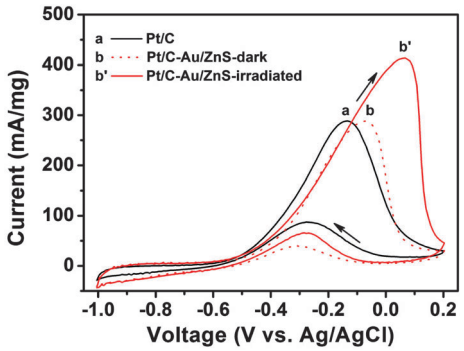

Fig. 3 CVs of methanol oxidation on pristine Pt/C and composite Pt/C-Au/ZnS-1 catalysts under different measurement conditions.

Pt/C as the anode catalyst (denoted as Pt/C–Au/ZnS), a CV profile resembling that of pristine Pt/C but with a suppressed backward peak was recorded in the dark. This phenomenon implies that in a dark environment Au/ZnS nanocrystals affected the methanol electrocatalysis of Pt/C by facilitating the removal of the adsorbed CO species. We surmised that the hydroxides formed at the shell surface of Au/ZnS nanocrystals in alkaline solution[18] may provide activated oxygen moieties for oxidation of CO residuals, thus expediting their removal from the catalyst surface to improve CO tolerance.[19] The beneficial effect of Au/ZnS incorporation can be further augmented by applying light irradiation during the process of methanol electrocatalysis. As displayed in Fig. 3, under light illumination the composite catalyst of Pt/C–Au/ZnS showed a remarkably enhanced peak current of methanol oxidation. The measured peak current value for Pt/C–Au/ZnS was 412.4 mA mg^{-1}, around 43.3% improvement over the pristine Pt/C catalyst. To understand the mechanism of performance enhancement for Pt/C–Au/ZnS in methanol electrocatalysis, we collected the CV data by using Au/ZnS nanocrystals as the exclusive anode catalyst. As shown in Fig. S7,† Au/ZnS alone did not show recognizable methanol oxidation peaks under light illumination, suggesting that methanol electrocatalysis was not initiated by illuminated Au/ZnS in the applied voltage range of −1.0–0.2 V *vs.* Ag/AgCl. This phenomenon can be realized by the fact that relatively limited amounts of holes were photogenerated in Au/ZnS nanocrystals during the very short period of CV measurement (about 2 min for an entire scan), with which methanol oxidation was hardly catalyzed to generate detectable anodic currents. The instead noticeable methanol oxidation peaks recorded on Au/ZnS under an extended irradiation time during CV measurement may support the above contention. When employing Pt/C–Au/ZnS as the anode catalyst, methanol oxidation can be readily triggered by Pt/C in the forward scan, which was subsequently promoted by the additional photogenerated holes of Au/ZnS. Since Au/ZnS nanocrystals incorporated at the anode additionally oxidized methanol under light illumination, an enhancement in anodic current generation resulted. This outcome demonstrates that Au/ZnS nanocrystals may boost the performance of DMFCs by providing supplementary photogenerated holes for participation in anodic methanol oxidation under light illumination. In addition, the photoexcited electrons transferring to the Au core may be extracted to contribute to the current generation as well. Since an appropriate bias potential was needed in order to drive away the localized electrons at Au, an increased peak potential of methanol oxidation was expected as observed on Pt/C–Au/ZnS. It should be noted that although incorporating Au/ZnS nanocrystals at the anode increased peak potential of methanol oxidation under light illumination, significant current enhancement can be achieved with only half-loading of Pt/C, which is essentially practical from the economical point of view.

In conclusion, we presented the photocatalytic properties of Au/ZnS core/shell nanocrystals toward methanol oxidation and demonstrated their use as the anode photocatalyst in the half-cell reaction of DMFCs. The results showed that incorporation of Au/ZnS nanocrystals not only resolved the CO poisoning issue for the Pt/C catalyst, but also enhanced the current generation of methanol oxidation under light illumination. The current study describes a new configuration of highly efficient photo-assisted DMFCs in which methanol oxidation at the anode is carried out electrocatalytically on a precious metal and photocatalytically on metal/semiconductor hybrid nanocrystals.

This work was financially supported by the National Science Council of Republic of China (Taiwan) under grants NSC-100-2113-M-009-004, NSC-101-2113-M-009-018, and NSC-101-3113-P-009-005.

Notes and references

1 (*a*) V. M. Dhavale and S. Kurungot, *J. Phys. Chem. C*, 2012, **116**, 7318–7326; (*b*) K. K. Haldar, G. Sinha, J. Lahtinen and A. Patra, *ACS Appl. Mater. Interfaces*, 2012, **4**, 6266–6272.
2 (*a*) A. Kostopoulou, F. Thétiot, I. Tsiaoussis, M. Androulidaki, P. D. Cozzoli and A. Lappas, *Chem. Mater.*, 2012, **24**, 2722–2732; (*b*) K. S. Lee, R. M. Anisur, K. W. Kim, W. S. Kim, T.-J. Park, E. J. Kang and I. S. Lee, *Chem. Mater.*, 2012, **24**, 682–687.
3 J.-S. Lee, M. I. Bodnarchuk, E. V. Shevchenko and D. V. Talapin, *J. Am. Chem. Soc.*, 2010, **132**, 6382–6391.
4 (*a*) E. Shaviv, O. Schubert, M. A. Santos, G. Goldoni, R. D. Felice, F. Vallee, N. D. Fatti, U. Banin and C. Sonnichsen, *ACS Nano*, 2011, **5**, 4712–4719; (*b*) L. Zhang, D. A. Blom and H. Wang, *Chem. Mater.*, 2011, **23**, 4587–4598; (*c*) M. Li, X.-F. Yu, S. Liang, X.-N. Peng, Z.-J. Yang, Y.-L. Wang and Q.-Q. Wang, *Adv. Funct. Mater.*, 2011, **21**, 1788–1794.
5 (*a*) P. Li, Z. Wei, T. Wu, Q. Peng and Y. Li, *J. Am. Chem. Soc.*, 2011, **133**, 5660–5663; (*b*) L. Sun, D. Zhao, Z. Song, C. Shan, Z. Zhang, B. Li and D. Shen, *J. Colloid Interface Sci.*, 2011, **363**, 175–181.
6 J. Yang, D. Wang, H. Han and C. Li, *Acc. Chem. Res.*, 2013, DOI: 10.1021/ar300227e.
7 (*a*) J. Guo, H. Lou and X. Zheng, *Carbon*, 2007, **45**, 1314–1321; (*b*) N. Sun, X. Wen, F. Wang, W. Peng, N. Zhao, F. Xiao, W. Wei, Y. Sun and J. Kang, *Appl. Surf. Sci.*, 2011, **257**, 9169–9176.
8 N. Zhang, S. Liu and Y.-J. Xu, *Nanoscale*, 2012, **4**, 2227–2238.
9 K. Drew, G. Girishkumar, K. Vinodgopal and P. V. Kamat, *J. Phys. Chem. B*, 2005, **109**, 11851–11857.
10 S. Chen and L.-W. Wang, *Chem. Mater.*, 2012, **24**, 3659–3666.
11 (*a*) A. Wood, M. Giersig and P. Mulvaney, *J. Phys. Chem. B*, 2001, **105**, 8810–8815; (*b*) V. Subramanian, E. E. Wolf and P. V. Kamat, *J. Am. Chem. Soc.*, 2004, **126**, 4943–4950.
12 (*a*) W.-T. Chen, T.-T. Yang and Y.-J. Hsu, *Chem. Mater.*, 2008, **20**, 7204–7206; (*b*) T.-T. Yang, W.-T. Chen, Y.-J. Hsu, K.-H. Wei, T.-Y. Lin and T.-W. Lin, *J. Phys. Chem. C*, 2010, **114**, 11414–11420.
13 J. Turkevich, P. C. Stevenson and J. Hillier, *Discuss. Faraday Soc.*, 1951, **11**, 55–75.
14 (*a*) S. Pradhan, D. Ghosh and S. Chen, *ACS Appl. Mater. Interfaces*, 2009, **1**, 2060–2065; (*b*) A. A. Ismail, D. W. Bahnemann, I. Bannat and M. Wark, *J. Phys. Chem. C*, 2009, **113**, 7429–7435.
15 G. Wu, T. Chen, W. Su, G. Zhou, X. Zong, Z. Lei and C. Li, *Int. J. Hydrogen Energy*, 2008, **33**, 1243–1251.
16 T. Nash, *Atmos. Environ.*, 1967, **1**, 679–687.
17 T. Moehl, M. Abd El Halim and H. Tributsch, *J. Appl. Electrochem.*, 2006, **36**, 1341–1346.
18 A. Chatterjee, A. Priyam, S. C. Bhattacharya and A. Saha, *Colloids Surf., A*, 2007, **297**, 258–266.
19 P. A. Adcock, S. V. Pacheco, K. M. Norman and F. A. Uribe, *J. Electrochem. Soc.*, 2005, **152**, A459–A466.

